

# ChemComm

Accepted Manuscript



This is an *Accepted Manuscript*, which has been through the Royal Society of Chemistry peer review process and has been accepted for publication.

*Accepted Manuscripts* are published online shortly after acceptance, before technical editing, formatting and proof reading. Using this free service, authors can make their results available to the community, in citable form, before we publish the edited article. We will replace this *Accepted Manuscript* with the edited and formatted *Advance Article* as soon as it is available.

You can find more information about *Accepted Manuscripts* in the [Information for Authors](#).

Please note that technical editing may introduce minor changes to the text and/or graphics, which may alter content. The journal's standard [Terms & Conditions](#) and the [Ethical guidelines](#) still apply. In no event shall the Royal Society of Chemistry be held responsible for any errors or omissions in this *Accepted Manuscript* or any consequences arising from the use of any information it contains.

## COMMUNICATION

# Functionalizing with Glycopeptide Dendrimers Significantly Enhances the Hydrophilicity of the Magnetic Nanoparticles

Cite this: DOI: 10.1039/x0xx00000x

Received 00th January 2012,  
Accepted 00th January 2012Jinan Li,<sup>ab</sup> Fangjun Wang<sup>\*a</sup>, Jing Liu,<sup>ab</sup> Zhichao Xiong,<sup>ab</sup> Guang Huang,<sup>ab</sup>  
Hao Wan,<sup>ab</sup> Zheyi Liu,<sup>ab</sup> Kai Cheng,<sup>ab</sup> and Hanfa Zou<sup>\*a</sup>

DOI: 10.1039/x0xx00000x

www.rsc.org/

**Magnetic nanoparticles functionalized with maltosylated glycopeptide dendrimers were prepared via azide-alkynyl click reaction. The functionalized magnetic nanoparticles exhibited high hydrophilicity and good efficiency in glycopeptides enrichment by HILIC.**

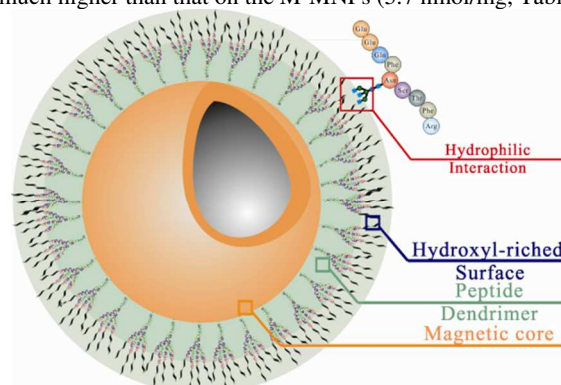
Various nanomaterials have been rapidly developed in recent years and play more and more important roles in biomedical and biotechnological areas.<sup>1</sup> For example, the magnetic nanoparticles are widely applied in magnetic-field-assisted bioseparation, biointeraction, imaging and drug delivery, due to their large surface area and easy manipulation by an external magnetic force.<sup>2</sup> However, further enhancement of the biological compatibility, hydrophilicity (water solubility) and the density of functional groups of these nanomaterials is still crucial to their applications, especially for the *in vivo* application.<sup>3</sup> Thus polyethylene glycol (PEG)<sup>4</sup> and organic polymer dendrimer<sup>5</sup> have been applied for the modification of nanomaterials in recent years.

Glycopeptide dendrimers consist of branched oligopeptide trees with glycosidic groups, and its hydrophilicity and binding capacity can be adjusted by varying the amino acid constitutes and attached glycans structures. Compared to other organic polymer dendrimers, the glycopeptide dendrimers exhibit lower toxicity, higher flexibility and higher biocompatibility owing to natural amino acid building blocks.<sup>6</sup> The glycopeptide dendrimers have been feasibly applied in biomedical areas, such as drug delivery and inhibiting cell surface protein-carbohydrate interactions for their high biological compatibility and multivalent binding sites.<sup>7</sup> Reymond et al. applied the galactosylated and fucosylated glycopeptide dendrimers as potent *P. aeruginosa* biofilm inhibitors with multivalent ligands targeting the galactose- or fucose-specific lectin Lec A or Lec B, and they demonstrated the multivalency of glycopeptide dendrimers was crucial for biofilm inhibition and dispersal with the functional groups.<sup>6</sup>

In this study, a second generation maltosylated glycopeptide dendrimer was functionalized onto the magnetic nanoparticles. The nanoparticles (dM-MNPs) were synthesized by immobilizing branched N<sub>3</sub>-oligopeptides onto the surface of magnetic nanoparticles, followed by functionalization with maltose via click chemistry (Scheme 1 and Scheme S1, ESI†).<sup>8</sup> The characteristics of

dM-MNPs are: (1) magnetic core with a strong magnetic response for the ease separation; (2) a silica layer is assembled onto the magnetic core for the improvement of the hydrophilicity of material surface and the easiness of post-functionalization; (3) branched peptide backbones with high biological compatibility and structure flexibility are immobilized onto the silica layer; (4) a large amount of maltose are grafted onto the surface of nanoparticles due to the high efficiency of click chemistry and the multivalency of peptide dendrimers. Magnetic nanoparticles directly modified with "click maltose" without peptide dendrimers (M-MNPs) were also synthesized for comparison (Scheme S1, ESI†).

As shown in Fig. 1A, the dM-MNPs exhibited a well-defined core-shell structure (core, ca. 170 nm) and good superparamagnetic property with a magnetization saturation value of 49.7 emu/g (Fig. 1B), and it took only several seconds to separate the dM-MNPs from biological matrix by magnet. In the FT-IR spectra (Fig. 1C), the appearance of bands at 1640 cm<sup>-1</sup> (C=O stretching, amide), 2855 cm<sup>-1</sup> (C-H stretching), 1450 cm<sup>-1</sup> (C-H bending) and 2110 cm<sup>-1</sup> (<sup>+</sup>N=N=N<sup>-</sup> antisymmetric stretching) revealed the successful conjugation of N<sub>3</sub>-pepdendrimer onto the SiO<sub>2</sub> layer. The disappearance of 2110 cm<sup>-1</sup> band (Fig. 1C) confirmed the growth of 1-propargyl-O-maltose on the surface of nanoparticles by click chemistry. In addition, elemental analysis determined that the amount of maltose  $\chi_{\text{maltose}}$  on the dM-MNPs was 89 nmol/mg, which was much higher than that on the M-MNPs (5.7 nmol/mg, Table 1).



**Scheme 1.** The structure of dM-MNPs and the hydrophilic interaction between dM-MNPs and N-glycopeptide.

**Table 1** Elemental analysis of four functionalized MNPs.

MNP	C (%)	N (%)	H (%)	$\chi_{\text{maltose}}^a/\text{nmol mg}^{-1}$
MNPs-dN <sub>3</sub>	13.44	2.957	1.152	-
dM-MNPs	14.95	3.424	2.049	89.88
MNPs-N <sub>3</sub>	3.920	0.953	0.721	-
M-MNPs	4.016	0.326	0.551	5.71

<sup>a</sup>The amount of maltose was calculated based on the carbon content from element analysis according to Eq. S1.<sup>4,9</sup>

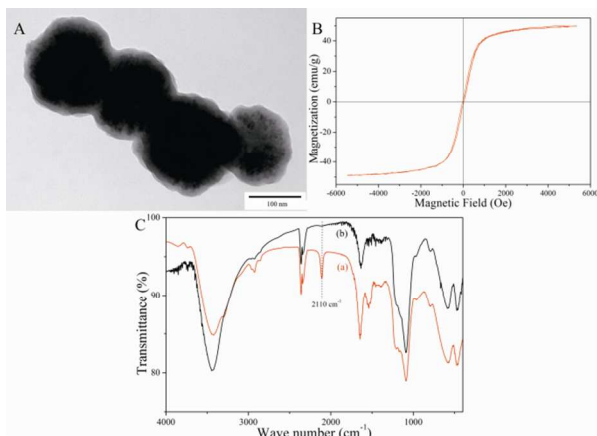


**Fig. 1** (A) TEM image and (B) hysteresis loop of dM-MNPs, (C) FT-IR spectra of (a) MNPs-dN<sub>3</sub> and (b) dM-MNPs.

Thus the amount of immobilized maltose was increased about 15 times by introducing peptide dendrimers onto the material surface, and this may be owing to the elimination of steric effect, since the maltose were far-removed from the surface of magnetic nanoparticles and the peptide backbones were highly flexible.<sup>10</sup>

Then, the hydrophilicity of the dM-MNPs and M-MNPs was evaluated by the water contact angle analysis. Compared with the M-MNPs, the water contact angle of dM-MNPs markedly decreased (Fig. S2, ESI<sup>†</sup>), demonstrating the hydrophilicity was clearly improved due to the 15 times increase of maltose immobilization amount. Thus we speculated the hydrophilic interaction between dM-MNPs and other hydrophilic biomolecules may be also enhanced because of the increase of material hydrophilicity, the elimination of steric effect by the flexible peptide backbones and the multivalent maltose cooperation with each other during the interaction with other biomolecules.<sup>11</sup> Firstly, the binding property of the dM-MNPs and M-MNPs with horseradish peroxidase (HRP), a typical glycoprotein with the mass of 44 kDa and 9 glycosylation sites, was determined by using UV-vis spectrophotometer.<sup>5b</sup> As shown in Fig. S3, the binding amount of HRP onto dM-MNPs was evidently higher than that onto M-MNPs. After equilibrium, the maximum binding capacity of dM-MNPs was about 6 mg/g (HRP/dM-MNPs), which was about 5 times higher than M-MNPs (1 mg/g, HRP/ M-MNPs). Meanwhile, the dM-MNPs were applied to direct capture of *N*-glycopeptides from the tryptic digests of human serum IgG (Scheme S2, ESI<sup>†</sup>). Briefly, 3  $\mu\text{g}$  IgG digests was mixed with different amounts of dM-MNPs and gently vortexed for 30 min, followed by the analysis of the eluted *N*-glycopeptides with MALDI-TOF MS. The peak intensity of 6 selected *N*-glycopeptides was set as indicators.<sup>4</sup> Obviously, the intensity of the 6 peaks mainly reached maximum when 20  $\mu\text{g}$  of dM-MNPs was applied (Fig. S4A, ESI<sup>†</sup>). Therefore, the *N*-glycopeptides within 3  $\mu\text{g}$  IgG digest can be almost captured by 20  $\mu\text{g}$  of dM-MNPs and the binding capacity of dM-MNPs was about 150 mg/g (IgG/dM-MNPs). In contrast, 120  $\mu\text{g}$  of M-MNPs were needed to fully capture the same 6 *N*-glycopeptides at identical condition and the binding capacity was about 25 mg/g (IgG/M-MNPs) (Fig. S4B, ESI<sup>†</sup>). Thus the *N*-glycopeptide binding capacity also increased 5 times for dM-MNPs over the M-MNPs. Above results clearly demonstrated that the hydrophilic interaction

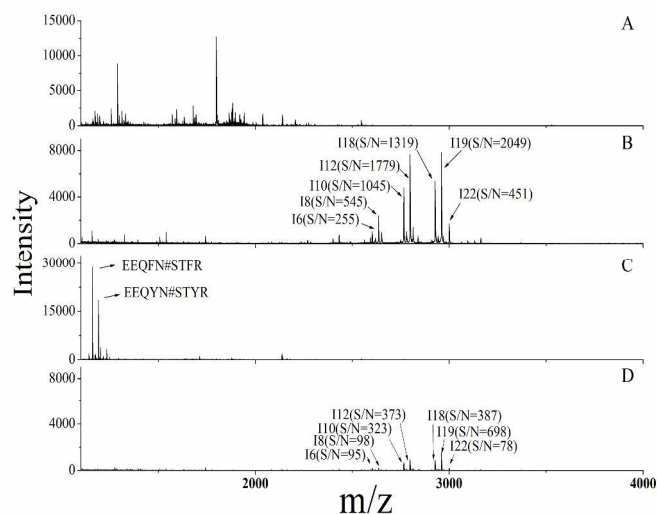


**Fig. 2** MALDI-TOF MS spectra of 0.5 pmol tryptic digest of human IgG. (A) direct analysis, (B) after enrichment by dM-MNPs and (C) deglycosylation by PNGase F, (D) after enrichment by M-MNPs.

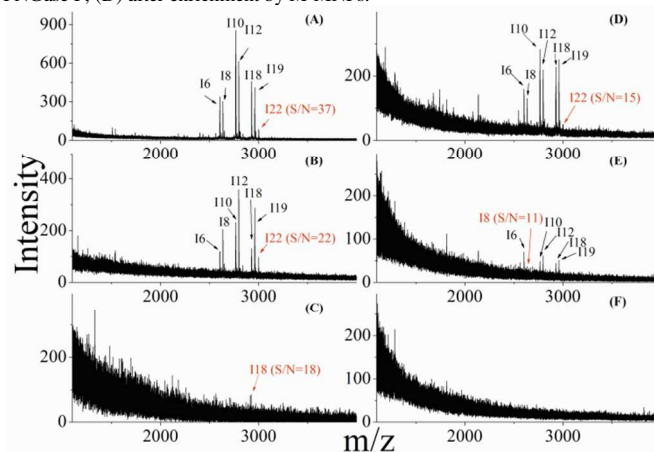


**Fig. 3** MALDI-TOF MS spectra of (A) 50 fmol, (B) 5 fmol and (C) 0.1 fmol tryptic digest human IgG after enrichment by dM-MNPs, (D) 50 fmol, (E) 5 fmol and (F) 0.1 fmol tryptic digest human IgG after enrichment by M-MNPs.

between dM-MNPs and hydrophilic glycopeptides or glycoproteins is significantly enhanced in our study, which was consistent with our speculation as mentioned above.

The enhanced hydrophilic interaction between dM-MNPs and *N*-glycopeptides is crucial to improve the efficiency of specific enrichment of *N*-glycopeptides, which is important for highly efficient *N*-glycosylation analyses of complex biological samples. Direct analysis of the tryptic digests of IgG revealed that the signals of *N*-glycopeptides ( $m/z > 2398.3$ ) were seriously suppressed by those highly abundant non-glycopeptides (Fig. 2A). In contrast, after enrichment by hydrophilic dM-MNPs, non-glycopeptides signals were dramatically eliminated and the *N*-glycopeptides were clearly detected with high intensity and signal to noise ratio (S/N) (Fig. 2B). Further, the enriched *N*-glycopeptides were deglycosylated by PNGase F and all the peaks of *N*-glycopeptides were disappeared and only two deglycosylated peptides ( $m/z = 1158.5, 1190.5$ ) were detected, which is consistent with previous works.<sup>4,12</sup> The detailed structures of *N*-glycopeptides captured by dM-MNPs are listed in Table S1. Compared with dM-MNPs, both the intensity and S/N of *N*-glycopeptides captured by M-MNPs were much lower (Fig. 2D). Then, 50, 5 and 0.1 fmol tryptic digests of IgG were utilized to investigate the detection limit of dM-MNPs and M-MNPs. It was observed that at least 6 *N*-glycopeptides with high S/N ratio were

detected by using dM-MNPs for 50 and 5 fmol IgG (Fig. 3A and B), and 1 *N*-glycopeptide ( $m/z=2926.5$ ) could be detected with S/N value of 18 for 0.1 fmol IgG (Fig. 3C). However, only 5 *N*-glycopeptides with much lower S/N ratio were detected in the case of M-MNPs for 50 and 5 fmol IgG (Fig. 3D and E), and no *N*-glycopeptide signal was observed for 0.1 fmol IgG (Fig. 3F). Furthermore, the dM-MNPs also exhibited good enrichment recovery (78-92%) for the glycopeptides (Table S2, ESI†).

Inspired by aforementioned results, the dM-MNPs were further applied to the capture of *N*-glycopeptides from 80  $\mu$ g tryptic digests of complex protein sample extracted from mouse liver. Totally, 1 083 *N*-glycosylation sites from 1 009 *N*-glycopeptides of 572 *N*-glycoproteins were identified in three independent analyses (Table S3, ESI†). Whereas only 693 *N*-glycosylation sites from 653 *N*-glycopeptides of 418 *N*-glycoproteins were obtained by using M-MNPs (Fig. S5, ESI†). Obviously, the dM-MNPs exhibited much better performance than M-MNPs and 56% more *N*-glycosylation sites could be characterized. In addition, about 90% of the results obtained by M-MNPs were covered by dM-MNPs (Fig. S6, ESI†), and intensity ratios of 83% *N*-glycopeptides identified with enrichment by dM-MNPs over M-MNPs were >1.5 (Table S4, ESI†). Above results clearly demonstrated that the enhanced hydrophilic interaction between dM-MNPs and hydrophilic biomolecules notably improved the *N*-glycopeptides enrichment efficiency for both standard and complex protein samples, which showed the great potential application in the glycoproteomes.

## Conclusions

In summary, the magnetic nanoparticles functionalized with glycopeptide dendrimers were prepared in this study for the first time. We found the hydrophilic interaction between dM-MNPs and hydrophilic biomolecules was significantly enhanced when compared with M-MNPs in view of the following reasons: (1) the amount of immobilized maltose was improved 15 times attributed to the multivalency of peptide dendrimers, which led to the visible increase of the material hydrophilicity; (2) the branched peptide backbones exhibited high biological compatibility, high flexibility and elimination of the steric effect; (3) the multivalent maltose may cooperate with each other during the hydrophilic interaction with other biomolecules to boost binding capability. The glycopeptide and glycoprotein capturing capacity were both improved 5 times by using the dM-MNPs over M-MNPs, and good enrichment recovery (78-92%) and detection limit as low as 0.1 fmol glycopeptide was feasibly achieved in this study. Therefore, the glycopeptide dendrimers functionalized magnetic nanoparticles are ideal materials with multivalent binding sites, enhanced hydrophilicity, good biological compatibility and easiness in operation. With all these advances, we believe it can be utilized in many biomedical and biotechnological areas in the future.

## Acknowledgements

Financial support from the China State Key Basic Research Program Grant (2013CB911203, 2012CB910601), the Creative Research Group Project of NSFC (21321064), the National Natural Science Foundation of China (21235006, 81161120540, 21305139).

## Notes and references

<sup>a</sup> CAS Key Laboratory of Separation Sciences for Analytical Chemistry, National Chromatographic R&A Center, Dalian Institute of Chemical Physics, Chinese Academy of Sciences (CAS), Dalian 116023, China;

<sup>b</sup> University of Chinese Academy of Science, Beijing 100049, China.

\* E-mail: wangfj@dicp.ac.cn, hanfazou@dicp.ac.cn

†Electronic Supplementary Information (ESI) available: Experiment details, supporting Fig.s and tables. See DOI: 10.1039/b000000x/

- 1 (a) Y. Fang, G. Zheng, J. Yang, H. Tang, Y. Zhang, B. Kong, Y. Lv, C. Xu, A. M. Asiri, J. Zi, F. Zhang, D. Zhao, *Angew. Chem. Int. Ed.* 2014, **53**, 5366-5370; (b) W. Wei, X. He, N. Ma, *Angew. Chem. Int. Ed.* 2014, **126**, 5679-5683; (c) C. N. Lui, Y. P. Tsui, A. S. Ho, D. K. Shum, Y. S. Chan, C. T. Wu, H. W. Li, S. C. Tsang, K. K. Yung, *Angew. Chem. Int. Ed.* 2013, **52**, 12298-12302.
- 65 2 (a) H. Wan, H. Qin, Z. Xiong, W. Zhang, H. Zou, *Nanoscale* 2013, **5**, 10936-10944; (b) S. Shylesh, V. Schunemann, W. R. Thiel, *Angew. Chem. Int. Ed.* 2010, **49**, 3428-3459; (c) J. Kim, Y. Piao, N. Lee, Y. I. Park, I. H. Lee, J. H. Lee, S. R. Paik, T. Hyeon, *Adv. Mater.* 2010, **22**, 57-60; (d) S. Giri, B. G. Trewyn, M. P. Stellmaker, V. S. Lin, *Angew. Chem. Int. Ed.* 2005, **44**, 5038-5044; (e) J. Kim, H. S. Kim, N. Lee, T. Kim, H. Kim, T. Yu, I. C. Song, W. K. Moon, T. Hyeon, *Angew. Chem. Int. Ed.* 2008, **47**, 8438-8441; (f) S. J. Son, J. Reichel, B. He, M. Schuchman, S. B. Lee, *J. Am. Chem. Soc.* 2005, **127**, 7316-7317.
- 75 3 (a) Z. Li, L. Wei, M. Y. Gao, H. Lei, *Adv. Mater.* 2005, **17**, 1001-1005; (b) L. H. Reddy, J. L. Arias, J. Nicolas, P. Couvreur, *Chem. Rev.* 2012, **112**, 5818-5878; (c) L. Wang, Z. Yang, J. Gao, K. Xu, H. Gu, B. Zhang, X. Zhang, B. Xu, *J. Am. Chem. Soc.* 2006, **128**, 13358-13359.
- 80 4 Z. Xiong, L. Zhao, F. Wang, J. Zhu, H. Qin, R. Wu, W. Zhang, H. Zou, *Chem. Commun.* 2012, **48**, 8138-8140.
- 85 5 (a) L. Zhang, H. Jiang, J. Yao, Y. Wang, C. Fang, P. Yang, H. Lu, *Chem. Commun.* 2014, **50**, 1027-1029; (b) H. Wang, Z. Bie, C. Lü, Z. Liu, *Chem. Sci.* 2013, **4**, 4298.
- 6 J. L. Reymond, M. Bergmann, T. Darbre, *Chem. Soc. Rev.* 2013, **42**, 4814-4822.
- 90 7 (a) S. K. Choi, A. Myc, J. E. Silpe, M. Sumit, P. T. Wong, K. McCarthy, A. M. Desai, T. P. Thomas, A. Kotlyar, M. M. Holl, B. G. Orr, J. R. Baker, Jr., *ACS Nano* 2013, **7**, 214-228; (b) R. U. Kadam, M. Bergmann, M. Hurley, D. Garg, M. Cacciarini, M. A. Swiderska, C. Nativi, M. Sattler, A. R. Smyth, P. Williams, M. Camara, A. Stocker, T. Darbre, J. L. Reymond, *Angew. Chem. Int. Ed.* 2011, **50**, 10631-10635; (c) D. Pati, N. Kalva, S. Das, G. Kumaraswamy, S. Sen Gupta, A. V. Ambade, *J. Am. Chem. Soc.* 2012, **134**, 7796-7802.
- 95 8 (a) D. A. Tomalia, A. M. Naylor, W. A. Goddard, *Angew. Chem. Int. Ed.* 1990, **29**, 138-175; (b) C. Rao, J. P. Tam, *J. Am. Chem. Soc.* 1994, **116**, 6975-6976.
- 100 9 C. E. Kibbey, M. E. Meyerhoff, *Anal. Chem.* 1993, **65**, 2189-2196.
- 10 (a) J. R. Kramer, T. J. Deming, *J. Am. Chem. Soc.* 2012, **134**, 4112-4115; (b) K. S. Krannig, H. Schlaad, *J. Am. Chem. Soc.* 2012, **134**, 18542-18545; (c) H. Lu, J. Wang, Y. Bai, J. W. Lang, S. Liu, Y. Lin, J. Cheng, *Nat. Commun.* 2011, **2**, 206.
- 105 11 (a) R. Breinbauer, E. N. Jacobsen, *Angew. Chem. Int. Ed.* 2000, **112**, 3750-3753; (b) C. Valério, J.-L. Fillaut, J. Ruiz, J. Guittard, J.-C. Blais, D. Astruc, *J. Am. Chem. Soc.* 1997, **119**, 2588-2589; (c) E. Delort, T. Darbre, J. L. Reymond, *J. Am. Chem. Soc.* 2004, **126**, 15642-15643.
- 110 12 Z. Xiong, H. Qin, H. Wan, G. Huang, Z. Zhang, J. Dong, L. Zhang, W. Zhang, H. Zou, *Chem. Commun.* 2013, **49**, 9284-9286.